THE ASTROPHYSICAL JOURNAL, 312:503–513, 1987 January 15

PROPERTIES OF THE X-RAY EMITTING GAS IN EARLY-TYPE GALAXIES

CLAUDE R. CANIZARES
Department of Physics and Center for Space Research, Massachusettes Institute of Technology
AND
GIUSEPPINA FABBIANO AND GINEVRA TRINCHIERI[1]
Harvard-Smithsonian Center for Astrophysics
Received 1986 March 17; accepted 1986 July 7

ABSTRACT

We have studied a sample of 81 E and S0 galaxies that were observed with the *Einstein Observatory*. Group membership and the effects of the infall toward the Virgo Cluster are accounted for in determining the distances to the galaxies. Fifty-five galaxies are detected in X-rays, most of which come from a hot interstellar medium. Discrete sources may make a significant contribution to the X-ray emission for 21 of the detected galaxies with the lowest X-ray luminosity L_X for a given optical luminosity L_B. We examine the L_X versus L_B distribution and derive approximate values of the central electron density, central cooling time, and total mass in gas for the sample. Typical values are ~ 0.1 cm^{-3}, $\sim 5 \times 10^6$ yr, and $5 \times 10^9\ M_\odot$. The short cooling times suggest the presence of cooling flows, and we consider heating by supernovae and by gravitational processes. Supernovae at the accepted rate would overproduce the observed X-ray luminosity: either the true rate is many times lower, or the supernova energy is not well coupled to the hot gas. There are also difficulties in explaining the suppression of a strong galactic wind if supernova heating dominates, unless an external pressure confines the gas. Gravitational heating gives $L_X \propto L_B\ \sigma^2$, where σ is the line-of-sight velocity dispersion in the galaxy, and we find that this is roughly the case. Gravitational heating exceeds the mean observed L_X by a factor of ~ 3–4 if one uses the accepted rate of stellar mass loss and assumes that the gas falls all the way to the center of the galaxy. This could be reconciled if the mass injection rate were lower or if matter drops out of the flow at all radii. The sample properties provide no additional information about the presence or absence of heavy halos in early-type galaxies.

Subject headings: galaxies: structure — galaxies: X-rays

I. INTRODUCTION

It is now well established that many early-type galaxies contain hot, X-ray emitting gas (Forman *et al.* 1979; Biermann, Kronberg, and Madore 1982; Biermann and Kronberg 1983; Nulsen, Stewart, and Fabian 1984; Dressel and Wilson 1985; Forman, Jones, and Tucker 1985, hereafter FJT; Trinchieri and Fabbiano 1985, hereafter TF; Stanger and Schwarz 1986; Canizares *et al.* 1986; Trinchieri, Fabbiano, and Canizares 1986, hereafter TFC; Stanger and Warwick 1986). FJT and TF studied largely overlapping samples containing 55 galaxies (including 5 Sa's) and 29 galaxies respectively and drew several general conclusions about the nature of the X-ray emission. For those X-ray luminous galaxies that are almost certain to contain hot gas, they find gas masses of $\sim 10^9$–$10^{10}\ M_\odot$, temperatures of $\sim 10^7$ K, and extents comparable to the optical radii of the galaxies. They also find that the X-ray luminosities of the sample galaxies are not simply proportional to their optical luminosities, but rather that $L_X \propto L_B^{1.7}$ (here L_X is the X-ray luminosity in a band of 0.5–4.5 keV and L_B is the blue luminosity of the galaxy).

Here we extend the analysis to an enlarged sample of 81 elliptical and S0 galaxies drawn from all the previously cited works and including 12 presented here for the first time. There are measured X-ray fluxes for 55 galaxies and upper limits for 26. We attempt to use consistent optical parameters for the galaxies, including a correction to the velocities for the Virgocentric flow. Then we use the sample to explore the contribution from discrete sources, the global physical properties of the hot gas, and the implications for heating by supernovae and gravity. Finally, we consider the question of the presence of heavy halos.

II. THE SAMPLE OF EARLY-TYPE GALAXIES

Table 1 lists all the relevant parameters for the galaxies in our sample. We include only galaxies that are classified as E or S0 by Sandage and Tammann (1981, hereafter RSA) or by de Vaucouleurs, de Vaucouleurs, and Corwin (1976, hereafter RC2). We have taken the measured X-ray fluxes from the references listed in the table (corrections of order 10% have been made to some entries to bring all data to the energy band 0.5–4.5 keV; also, for NGC 5128 we take the total "diffuse" luminosity listed in the text of FJT—see § III*a*). Data for 12 galaxies, five detections and seven upper limits, are reported here for the first time (the uncertainties in these fluxes are dominated by $\sim 20\%$–30% systematic effects). In addition, by using more refined (Rev. 1B) data we were able to detect two galaxies previously reported as upper limits (NGC 936 and NGC 4643) and to determine improved upper limits for three others (NGC 1574, NGC 3489, and NGC 3818). We believe that our sample includes nearly all the relatively isolated, reasonably normal, early-type galaxies that were observed with Einstein.

The total corrected blue magnitudes are taken from RSA when available or from RC2 (but corrected for extinction as in RSA). For the remaining nine galaxies, we use the magnitudes from Zwicky *et al.* (1968) and compute the total corrected blue magnitudes by following the RSA and de Vaucouleur and Pence (1979) with diameters taken from RC2 or Nilson (1973).

[1] Also Osservatoria Astrofisico di Arcetri.

TABLE 1

EARLY-TYPE GALAXIES

	Name	R.A.	DEC	Group[a]	V[b]	B mag	$10^{13}f_x$	ref	M_B	σ	$\log L_x$	$\log L_B$	$\log \Delta L_x$
		hh.mmss	dd.mmss		km/s		erg/cm^{2}s			km/s	erg/s	$L_\odot$	erg/s
1	N0205	0.3736	41.25	M31	34	8.60	< 20.00	1	-15.5	97	< 38.03	8.40	< 37.34
2	N0315	0.5506	30.05	GH8	5095	12.75	6.48	2	-22.3	273	41.91	11.11	41.88
3	N0524	1.2206	9.17	(GH13)	2427	11.62	2.40	2	-21.8	270	40.83	10.92	40.60
4	N0584	1.2850	-7.08		1855	11.20	0.89	4	-21.7	234	40.17	10.85	-----
5	N0720	1.5036	-13.59		1662	11.15	8.64	2	-21.5	224	41.06	10.78	40.97
6	N0936	2.2506	-1.23	(GH28)	1438	11.19	0.80	4	-21.1	193	39.90	10.63	-----
7	N0984	2.3154	23.12		4403	13.21	< 6.63	3	-21.5		< 41.79	10.80	< 41.77
8	N1167	2.5836	35.01		4951	13.40	< 4.43	3	-21.6		< 41.72	10.82	< 41.70
9	N1172	2.5918	-15.02		1598	13.00	< 0.79	2	-19.5	99	< 39.99	10.00	< 39.80
10	N1332	3.2406	-21.31	HG32	1518	11.29	5.02	2	-21.1	306	40.74	10.64	40.61
11	N1380	3.3430	-35.08	HG17	1309	11.10	4.34	2	-21.0	227	40.55	10.59	40.35
12	N1395	3.3618	-23.11	HG32	1518	11.18	6.92	2	-21.2	249	40.88	10.68	40.78
13	N1400	3.3715	-18.51		522	12.08	< 1.25	4	-18.0	269	< 39.21	9.40	< 38.90
14	N1407	3.3800	-18.44	HG32	1518	10.93	11.72	3	-21.5	274	41.11	10.78	41.04
15	N1497	3.5906	23.00		6198	13.70	< 5.32	3	-21.8		< 41.99	10.90	< 41.98
16	N1533	4.0848	-56.15	HG3	988	11.65	1.24	2	-19.8		39.76	10.12	39.12
17	N1574	4.2100	-57.05	HG3	988	11.13	< 2.30	4	-20.4		< 40.03	10.33	< 39.54
18	N1600	4.2912	-5.12		4687	12.01	6.14	2	-22.9	323	41.81	11.33	41.76
19	N2314	7.0348	75.19		3872	12.83	< 1.60	4	-21.6	301	< 41.06	10.84	< 40.96
20	N2300	7.1548	85.48	(HG92)	2337	11.99	4.78	2	-21.4	260	41.10	10.74	41.03
21	N2563	8.1742	21.14		4642	13.29	3.64	2	-21.6		41.58	10.81	41.55
22	N2629	8.4154	73.10	(HG89)	3648	12.30	< 2.00	4	-22.0	318	< 41.11	11.00	< 40.97
23	N2685	8.5142	58.56	(HG80)	1245	11.86	1.08	2	-20.1	102	39.91	10.24	39.33
24	N2693	8.5324	51.31		4865	12.70	< 1.8	4	-22.2	387	< 41.31	11.09	< 41.21
25	N2859	9.2118	34.44	(GH43)	2016	11.75	< 0.91	2	-21.3	179	< 40.25	10.70	< 38.77
26	N2974	9.4000	-3.28		2144	11.68	2.22	2	-21.5		40.69	10.78	40.45
27	N3078	9.5606	-26.41		2506	11.92	3.52	3	-21.6		41.03	10.82	40.92
28	N3115	10.0204	-7.29		506	9.89	< 1.85	4	-20.1	247	< 39.36	10.25	< -----
29	N3258	10.2636	-35.21	(HG18)	2808	12.48	4.99	2	-21.3		41.28	10.70	41.23
30	N3377	10.4506	14.15	GH68	875	11.10	< 2.09	2	-20.1	160	< 39.88	10.24	< 39.26
31	N3379	10.4512	12.51	GH68	875	10.33	< 3.20	1	-20.9	218	< 40.07	10.55	< -----
32	N3489	10.5742	14.10	GH68	875	11.13	< 1.70	4	-20.1	142	< 39.80	10.23	< 38.74
33	N3585	11.1212	60.58		1936	10.81	1.13	2	-22.1		40.31	11.04	-----
34	N3607	11.1418	18.20	GH77	1201	11.08	5.98	5	-20.8	240	40.62	10.52	40.48
35	N3818	11.3924	-5.52		1839	12.79	< 1.80	4	-20.0	196	< 40.47	10.21	< 40.38
36	N3894	11.4612	59.41	(GH91)	3257	12.63	< 3.81	3	-21.4	251	< 41.29	10.77	< 41.24
37	N3923	11.4830	-28.32	(HG28)	1887	10.79	5.95	2	-22.1	249	41.01	11.03	40.82
38	N3998	11.5518	55.44	GH94	1502	11.50	51.18	3	-20.9	308	41.74	10.55	41.73
39	N4105	12.0406	-29.29		2000	11.76	2.3	4	-21.3		40.65	10.69	40.44
40	N4203	12.1230	33.29	GH94	1502	11.62	20.00	4	-20.8	175	41.34	10.50	41.31
41	N4251	12.1536	28.27	GH94	1502	11.62	0.51	2	-20.8		39.74	10.50	-----
42	N4291	12.1806	75.40	(HG88)	2144	12.28	7.00	1	-20.9	295	41.19	10.54	41.15
43	N4365	12.2154	7.36	VIRGO	1285	10.60	2.45	2	-21.5	262	40.29	10.77	-----
44	N4374	12.2230	13.10	VIRGO	1285	10.23	7.72	2	-21.8	296	40.79	10.92	40.52
45	N4382	12.2254	18.28	VIRGO	1285	10.10	3.56	2	-22.0	200	40.45	10.97	-----
46	N4406	12.2342	13.13	VIRGO	1285	10.02	47.50	2	-22.0	256	41.58	11.00	41.53
47	N4459	12.2630	14.15	VIRGO	1285	11.49	1.56	2	-20.6	172	40.09	10.42	39.55
48	N4472	12.2712	8.17	VIRGO	1285	9.23	65.31	2	-22.8	315	41.71	11.32	41.65
49	N4473	12.2718	13.42	VIRGO	1285	11.07	1.13	2	-21.0	197	39.95	10.58	-----
50	N4477	12.2730	13.55	VIRGO	1285	11.24	1.37	2	-20.8	200	40.03	10.52	-----
51	N4550	12.3300	12.30	VIRGO	1285	12.33	< 0.89	2	-19.7	84	< 39.85	10.08	< 39.48
52	N4552	12.3306	12.50	VIRGO	1285	10.80	5.15	2	-21.3	273	40.61	10.69	40.38
53	N4564	12.3354	11.43	VIRGO	1285	11.87	< 0.87	2	-20.2	165	< 39.84	10.26	< 38.83
54	N4589	12.3530	74.28		2417	11.87	1.77	3	-21.6	241	40.70	10.81	40.44
55	N4621	12.3930	11.55	VIRGO	1285	10.67	1.16	4	-21.4	225	39.96	10.74	-----
56	N4636	12.4018	2.58	VIRGO	1285	10.50	55.63	2	-21.6	217	41.64	10.81	41.62
57	N4638	12.4018	11.43	VIRGO	1285	12.05	0.49	2	-20.0	133	39.59	10.19	-----
58	N4643	12.4048	2.15	VIRGO	1285	11.55	1.87	4	-20.5		40.17	10.39	39.81
59	N4649	12.4112	11.50	VIRGO	1285	9.83	31.67	2	-22.2	344	41.40	11.08	41.32
60	N4665	12.4236	3.20	VIRGO	1285	11.43	1.02	2	-20.6		39.91	10.44	-----
61	N4697	12.4600	5.32	VIRGO	1285	10.11	2.34	2	-21.9	186	40.27	10.97	-----
62	N4753	12.4948	-0.56	VIRGO	1285	10.85	1.55	2	-21.2		40.09	10.67	-----
63	N5077	13.1648	-12.24		2823	12.52	1.88	3	-21.2		40.86	10.69	40.74
64	N5102	13.1906	-36.22	(HG19)	169	10.47	< 3.11	2	-17.2	128	< 38.63	9.06	< 37.55
65	N5128	13.2230	-42.46		100	6.71	41.65	2	-19.8		39.30	10.11	-----
66	I4296	13.3348	-33.43		3629	11.43	4.02	2	-22.9	290	41.40	11.34	41.25
67	N5322	13.4736	60.26	GH122	2341	10.91	< 3.23	3	-22.4	310	< 40.93	11.17	< 40.54

TABLE 1—*Continued*

Name	R.A.	DEC	Group[a]	V[b]	B mag	$10^{13}f_X$	ref	M_B	σ	$\log L_X$	$\log L_B$	$\log \Delta L_X$
	hh.mmss	dd.mmss		km/s		erg/cm²s			km/s	erg/s	$L_\odot$	erg/s
68 N5318	13.4818	33.57		4179	13.31	< 2.89	3	-21.3		< 41.38	10.71	< 41.35
69 N5485	14.0527	55.14	GH132	2241	12.44	< 1.5	4	-20.8		< 40.56	10.52	< 40.40
70 I0989	14.1318	3.21		7570	13.80	< 2.75	3	-22.1		< 41.88	11.03	< 41.86
71 N5532	14.1424	11.02		7367	13.00	2.31	2	-22.8	294	41.78	11.33	41.72
72 N5846	15.0354	1.48	GH150	2032	11.13	36.04	6	-21.9	250	41.85	10.96	41.83
73 N5866	15.1048	55.58	(GH152)	1277	10.86	1.96	2	-21.2	170	40.19	10.66	-----
74 N5898	15.1530	-23.55		2103	12.41	1.56	2	-20.7		40.52	10.48	40.36
75 N6034	16.0112	17.20		10112	14.70	< 2.7	4	-21.8		< 42.12	10.92	< 42.11
76 N6146	16.2330	41.01		8738	13.51	< 0.27	3	-22.7	231	< 40.99	11.27	< 40.54
77 N6876	20.1306	-71.01		3951	12.45	0.47	2	-22.0		40.54	11.01	38.71
78 I1459	22.5424	-36.43	HG15	1373	10.96	3.31	2	-21.2		40.48	10.69	40.13
79 N7562	23.1324	6.25		3608	13.19	2.00	4	-21.1	288	41.10	10.63	41.04
80 N7619	23.1742	7.56	GH166	3489	12.17	7.12	7	-22.1	330	41.62	11.01	41.58
81 N7626	23.1812	7.57	GH166	3489	12.17	3.42	7	-22.1	270	41.30	11.01	41.22

[a] Group velocity used for those galaxies with group names not in parentheses.
[b] Hubble velocity (see text).
REFERENCES.—(1) Stanger and Schwarz 1986. (2) FJT. (3) Dressel and Wilson 1985. (4) This paper. (5) Biermann *et al.* 1982. (6) Biermann and Kronberg 1983. (7) Canizares *et al.* 1986.

All but two of these magnitudes are within 0.2 mag of the value m(Zw) − 0.4 mag, which is an approximate relation between the Zwicky magnitude m(Zw) and the total blue magnitude (J. Huchra private communication). The two most discrepant values are for NGC 984 and NGC 1497, which have only nonrestrictive X-ray upper limits and so are not of great interest in this work. For NGC 5128 (Cen A) we take the estimated magnitude of the elliptical galaxy component corrected for extinction by its own dust and for redenning in the Galaxy from Dufour *et al* (1979).

We obtain distances to the galaxies as follows. First, for those galaxies assigned to groups with more than 10 members by Geller and Huchra (1983) and Huchra and Geller (1982) we adopt the group velocity (the velocities listed in these references are corrected for a simple dipole Virgocentric flow model—we use these to compute heliocentric velocities). All galaxies within a 6° radius of M87 are assigned to the Virgo Cluster. For all galaxies not in groups or clusters, we use heliocentric velocities from the Center for Astrophysics redshift survey kindly provided by J. Huchra.

All heliocentric velocities below 2000 km s^{-1} are corrected for rotation of the Galaxy, motion relative to the center of the Local Group, and the infall to Virgo. This is accomplished with the algorithm of Aaronson *et al.* (1982) using an infall velocity of 250 km s^{-1} (see also Tammann and Sandage 1985). There are two galaxies treated as special cases: for NGC 5128 (Centaurus A) the Hubble flow velocity is set to 100 km s^{-1} to yield a distance of 2 Mpc following Davies *et al.* (1984; private communication); for NGC 205 we adopt a Hubble flow velocity of 34 km s^{-1} to give a distance of 680 kpc (Allen 1973).

Distances are computed from the final Hubble flow velocities using a Hubble constant of 50 km s^{-1} Mpc^{-1}, which is the value used in most of the previous papers on X-rays from elliptical galaxies. Note that because of the infall toward Virgo, this gives a distance of ~25 Mpc to the Virgo Cluster galaxies. Use of a larger Hubble constant would change the absolute luminosities of the galaxies but leave the relative properties of the sample unchanged. The use of the Virgo flow model has little qualitative effect on our conclusions, as we show explicitly in § III*b*.

The distances are used to compute absolute blue magnitudes

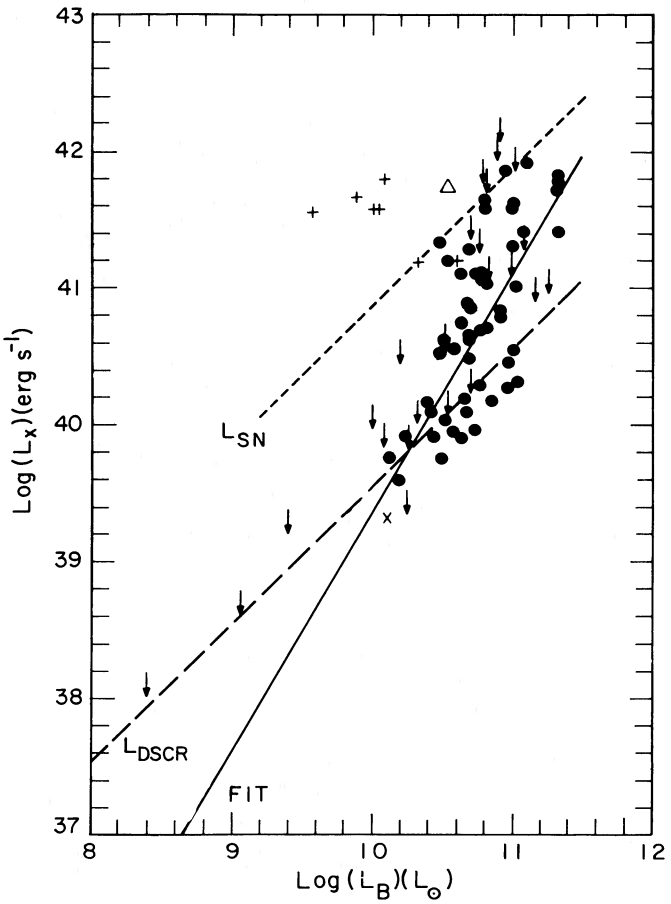

FIG. 1.—X-rays vs. optical (blue) luminosity of early-type galaxies. The filled circles are detections, the downward arrows upper limits. The possibly active galaxy NGC 3998 is shown as a triangle, and NGC 5128 (Cen A) is shown as a cross. The pluses are for the galaxies identified by Bechtold *et al.* (1983), which we have not included in our sample for reasons described in the text. The long-dashed line gives L_{dscr}, the estimate of the possible X-ray luminosity from discrete sources. The solid line is the mean L_X vs. L_B fit to the full sample, and the short-dashed line shows L_{SN}, the luminosity expected from heating by supernovae at the accepted rate, assuming all the energy emerges as X-rays.

M_B, blue luminosities in solar units (defined as $L_B = \text{dex}\,[-0.4\,(M_B - 5.41)]$), and X-ray luminosities.

III. THE GALAXIES IN A1367

We have chosen to exclude from our sample the galaxies which were associated with X-ray sources by Bechtold *et al.* (1983) in the cluster A1367. These authors found several regions of enhanced X-ray emission in the cluster with size scales of $\sim 1'$, mostly at 3–4 σ significance. For nine of these they associated the emission with cluster galaxies (two Sa's, the rest E or S0); four had no obvious galactic counterparts. As shown in Figure 1, at least five of the seven early-type galaxies identified in A1367 have X-ray luminosities that exceed those of the other galaxies with similar optical luminosity by nearly two orders of magnitude. If the emission from the vicinity of the A1367 galaxies is from a galactic gas similar to that in the other galaxies, it would imply that the cluster medium of A1367 is having a very significant effect on the galactic gas (FJT). However, the density of this medium is similar to that in the Virgo Cluster (Bechtold *et al.* 1983; Forman *et al.* 1979), where a large fraction of the other elliptical galaxies considered in this paper are located.

Another possibility is that the regions of enhanced X-ray emission found by Bechtold *et al.* (1983) may be due to clumpiness in the intracluster gas and should not be identified with gas in individual galaxies. The IPC image of A1367 shows a highly irregular X-ray surface brightness, with numerous local maxima on scales of $\sim 2'$–$5'$. Furthermore, several of the local maxima appear to be centered on groups of brighter galaxies, an association which is at least plausible if such a cluster is an amalgam of subgroups of galaxies and hot gas. Most of the enhancements found by Bechtold *et al.* are in these larger regions of bright, irregular cluster emission, which increases the probability of erroneously identifying a local maximum with a single galaxy.[2] The fact that in general the enhanced emission is not centered on the galaxy also undermines the identifications. Bechtold *et al.* considered most of these questions and concluded that galactic emission was still the most likely explanation. Upon re-examination, we believe that the identifications are not sufficiently secure to establish the existence of a class of galaxies with such discrepant X-ray to optical luminosity ratios.

IV. COMPARISON OF X-RAY AND OPTICAL PROPERTIES

Figure 1 shows a plot of the X-ray versus optical luminosity of all galaxies in the sample. Qualitatively, the distribution of points is similar to those in the corresponding plots of FJT and TF, although there are quantitative differences because of our different distance estimates. We note that none of the upper limits is restrictive, in that the data are consistent with the hypothesis that all early-type galaxies have X-ray luminosities that would fall within the locus of points in Figure 1. The most errant point is that for NGC 3998, which lies above the upper envelope of the remainder of the data. The higher than normal X-ray luminosity of NGC 3998 may well be due to the presence of an active galactic nucleus (see Dressel and Wilson 1985), in which case it would not be representative of normal early-type galaxies. We show it as a triangle in all the figures.

a) Discrete Source Contribution to L_X

Some of the X-ray emission from early-type galaxies must be due to discrete sources. The conclusions about thermal X-ray emission drawn from the L_X versus L_B distribution depend on the size of this discrete source component. TF estimated the contribution to L_X from globular cluster and binary X-ray sources and from single low-mass stars. They primarily used the observed luminosities of globular clusters and of sources in the bulge of M31, because its stellar content is indistinguishable from that of some elliptical galaxies such as NGC 4472 (see, e.g., Faber 1983; Oke, Bertola, and Capaccioli 1981; Bohlin *et al.* 1985). In scaling to other galaxies, they attempted to account for the possible effects of stellar density on the formation of X-ray binaries (see comments by Feigelson *et al.* 1981).

The estimated discrete source contribution to L_X, $L_{\rm dscr}$, scales approximately with optical luminosity. It is shown as a long-dashed curve in Figure 1. One might expect the contribution for any given galaxy to scatter by a factor of ~ 3 about this curve, which is the observed scatter in the X-ray to optical luminosity ratios for subclasses of spiral galaxies (Fabbiano and Trinchieri 1985). FJT conclude that the discrete source X-ray luminosity for an early-type galaxy of a given optical luminosity is at least a factor of 3 smaller than the dashed line of Figure 1. This is because they take one-half the observed luminosity of NGC 5128 (Cen A) as a strict upper limit (they adopt a distance of 5 Mpc from RSA, whereas we use 2 Mpc, but that does not affect the X-ray to optical luminosity ratio). We believe that all the diffuse emission from Cen A could be due to discrete sources, and in any case, the uncertainties in our estimate and the assumed spread in the distribution are sufficient to encompass both hypotheses.

The curve representing the estimated discrete source X-ray luminosity follows the lower envelope of the distribution of points in Figure 1. In fact the 19 X-ray detected galaxies that cluster about the curve appear to be slightly removed from the remainder of the distribution, suggesting that discrete sources could dominate their emission (the location of points relative to the line is independent of the assumed distances to the galaxies). All the galaxies with X-ray luminosities or upper limits within a factor of 2 of the dashed curve in Figure 1 are listed in Table 2.

We have not been successful in using the available data to decide whether discrete source emission is in fact dominant for the galaxies of Table 2. One potential discriminant is the X-ray spectrum, which could differentiate the $\sim 1 \times 10^7$ K thermal emission of hot gas from the higher temperature emission characteristic of discrete sources (e.g., the bulge sources of M31 have a mean temperature of 7–15×10^7 K; Fabbiano, Trinchieri, and van Speybroeck 1986). Unfortunately, the galaxies of Table 2 are too weak to permit this (e.g., the spectral fit for NGC 4382 in TFC is indeterminate). Even a joint fit to the data from several galaxies, which gives considerably improved statistical accuracy, cannot distinguish the two possibilities. We performed joint fits for six galaxies from Table 2 (NGC 1533,

[2] Four of the more significant ($\sim 5\ \sigma$) sources identified with galaxies Nos 27, 30, 33, and 53 are located in the brightest region of extended X-ray emission just to the southeast of the center of the cluster. Galaxy No. 33 is at the center of the bright plateau. Another source (7 σ, galaxy No. 18) is west of the cluster center in a region of very irregular emission with a secondary maximum; there are several other galaxies within $\sim 1'$–$2'$ of No. 18. Note that the sources without galaxy identifications are also in regions of irregular surface brightness, and at least two do not appear on the "filtered" high-resolution map from which some of the larger scale irregularities have been removed. In addition, because of the very irregular background, it is possible that the statistical significance of the sources has been over estimated (see e.g., Press and Schechter 1974).

TABLE 2

GALAXIES WITH POSSIBLY LARGE DISCRETE SOURCE COMPONENTS

Detections			
NGC 584	NGC 4365	NGC 4621	NGC 4753
NGC 936	NGC 4382	NGC 4638	NGC 5128
NGC 1533	NGC 4459	NGC 4643	NGC 5866
NGC 2685	NGC 4473	NGC 4665	NGC 6876
NGC 3585	NGC 4477	NGC 4697	IC 1459
NGC 4251			
Upper Limits			
NGC 205	NGC 3115	NGC 3489	NGC 5102
NGC 1400	NGC 3377	NGC 4550	NGC 5322
NGC 1574	NGC 3379	NGC 4564	NGC 6146
NGC 2859			

NGC 4365, NGC 4382, NGC 4697, NGC 6879, and IC 1459) and for seven apparently weak galaxies that fall well above the dashed curve of Figure 1 and therefore are probably dominated by thermal emission (NGC 534, NGC 720, NGC 1407, NGC 1600, NGC 3078, NGC 3923, and NGC 4203). Both fits simply constrain the mean temperature to be above 1.0×10^7 K (at 90% confidence), which is compatible with either thermal or discrete source emission. Low fluxes also preclude studying the X-ray surface brightness for clues about the origin of the emission (for some of the galaxies in Table 2, the surface brightness contours presented by FJT seem to show asymmetries, but these are of marginal statistical significance). Several of the galaxies in Table 2 show [N II] λ6584 emission (Phillips *et al.* 1985); if a connection can be established between such emission and the existence of a cooling flow (see § III*c*), then this would imply that the discrete source contribution is small.

In any case, it is unlikely that the contribution of discrete sources to the X-ray luminosity of early-type galaxies appreciably exceeds that indicated in Figure 1. So for a majority of galaxies, most if not all of the observed luminosity must have a different origin. The arguments favoring emission by hot gas are presented in FJT, TF, and references therein. In Figure 2 we show $\Delta L_X = L_X - L_{\rm dscr}$, the luminosity attributable to the gas if the discrete source contribution is as indicated by the dashed line in Figure 1. As one would expect, Figure 2 nearly reproduces the distribution of Figure 1 except for the points lying near the lower envelope. Therefore, most conclusions drawn from the properties of the distribution should be relatively independent of the assumptions about the discrete source component, as we discuss below.

Some of the galaxies in our sample have compact nuclear radio emission. The most luminous (NGC 315, NGC 5532 = 3C 296, IC 4296) have nuclear radio luminosities at 5 GHz of 10^{30}–10^{31} ergs s^{-1} Hz^{-1} (Bridle and Fomalont 1978; Fabbiano *et al.* 1984; Killeen, Bicknell, and Ekers 1986), which is at the low end of the distribution of luminosities of 3C radio galaxies. For these it is possible that nuclear X-emission could make a sizeable contribution to the X-ray luminosity (see, e.g., Elvis *et al.* 1981), although for IC 4296 the bulk of the X-ray emission clearly comes from an extended source (FJT; Killeen, Bicknell, and Carter 1986). These are among the most X-ray luminous galaxies, but they are also among the most optically luminous and do not depart from the distribution defined by the other galaxies, most of which have little or no radio emission. We have not included in our sample galaxies with nuclear

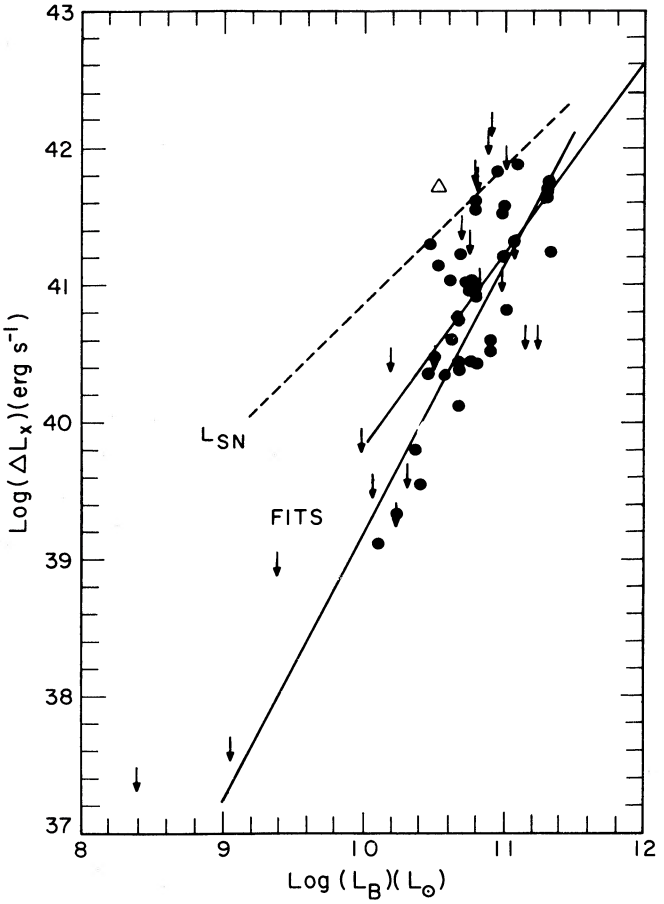

FIG. 2.—ΔL_X vs. optical luminosity, where $\Delta L_X = L_X - L_{\rm dscr}$. The symbols and the curve marked $L_{\rm SN}$ are as in Fig. 1. The longer of the two solid lines is the mean L_X vs. L_B fit from Table 3 for the full sample (excluding NGC 3993), and the shorter solid line is the fit to the subsample that excludes the galaxies in Table 2.

radio luminosities above 10^{31} ergs s^{-1} Hz^{-1}, for which the nuclear X-ray emission may be important (e.g., NGC 1218, which has nuclear radio luminosity $\sim 10^{32}$ ergs s^{-1} Hz^{-1} and total X-ray luminosity of 4×10^{42} ergs s^{-1}). For these reasons we have assumed that nuclear emission does not make a significant contribution to the X-ray luminosity of the galaxies in our sample. A detailed comparison of radio, X-ray and optical properties of early-type galaxies is given elsewhere (Fabbiano *et al.* 1987; see also Dressel and Wilson 1985).

b) Fits to the Distribution

As in TF, we performed a variety of fits to parameterize the distributions of Figures 1 and 2. We assumed that the conditional distribution function $P(l_1 \mid l_2)$ is a Gaussian with fixed standard deviation s and variable mean:

$$P(l_1 \mid l_2) = 1[\sqrt{(2\pi)}s] \exp\,[-(l_1 - \langle l_1 \rangle)^2/2s^2]\,, \qquad (1)$$

where

$$\langle l_1 \rangle = a + b(l_2 - c)\,. \qquad (2)$$

We use the maximum likelihood method of Avni *et al.* (1980) that incorporates both detections and upper limits to determine the free parameters a, b, and s. The constant c was fixed at a convenient value of l_2. In all the fits we excluded the A1367

TABLE 3

FITS TO THE DISTRIBUTION FUNCTION[a]

Parameter Sample	Number	b	b(68%)	b(90%)	a	s
Fits vs. $L_B(c = 11)$						
L_X (all)	80	1.73	1.52–1.98	1.42–2.11	41.05	0.48
ΔL_X (all)	59	1.93	1.72–2.19	1.58–2.31	41.10	0.52
Minus Table 2	46	1.39	1.20–1.68	0.95–1.85	41.19	0.39
Fits vs. $L_B\sigma^2(c = 16)$						
L_X (all)	56	1.19	1.06–1.38	0.95–1.43	41.22	0.49
ΔL_X (all)	41	1.30	1.13–1.47	1.04–1.60	41.22	0.56
Minus Table 2	32	0.82	0.61–1.03	0.49–1.19	41.24	0.42

[a] Fits are of the form $L_1 = a + b(L_2 - c)$.

galaxies and the possibly active galaxy NGC 3998. The results of the fits are given in Table 3.

The first row of Table 3 and the indicated curve in Figure 1 give the fit to total X-ray luminosity for the entire sample (less the possibly active galaxy NGC 3998), with $l_1 = \log(L_X)$, $l_2 = \log(L_B)$. The best-fit slope, 1.73, is very close to the value 1.64 found by TF for their smaller sample. If the discrete source contribution is much smaller than our estimate, then this fit gives the dependence of the hot gas luminosity on L_B; otherwise it is simply an empirical relation.

If the discrete source component is close to our estimate, then it is the residual X-ray luminosity ΔL_X of Figure 2 that represents the hot gas. We performed fits to the full sample of Figure 2 (less NGC 3998) and to a subset that excludes all the galaxies of Table 2. For these cases $l_1 = \log(\Delta L_X)$ and $l_2 = \log(L_B)$. The results are shown in Table 3 and Figure 2. The slopes are less well determined than for the fit to total X-ray luminosity but are in reasonable agreement with it. A linear dependence of the mean ΔL_X on L_B is marginally allowed for the fit to the full sample and is acceptable for the fit to the subsample.

For completeness we repeated all three fits using distances computed from heliocentric velocities for all the galaxies. All the best-fit slopes were smaller (by 0.1–0.4) but fell within one standard deviation of the values of Table 3.

We conclude that the dependence of mean X-ray luminosity on optical luminosity is steeper than linear, as found by FJT and TF, unless most of the galaxies in the lower portion of the distribution have significant contributions from discrete sources. In the latter case, the remaining distribution of ΔL_X versus L_B is rather amorphous and is consistent with a linear relation.

c) *Correlation with Optical Line Emission or Infrared Flux*

Phillips *et al.* (1985) and Véron-Cetty and Véron (1985) have recently undertaken surveys of [N II] λ6584 emission line strengths in the cores of elliptical galaxies. Emission lines are detected for 12 of the galaxies in our survey (including Cen A, for which the optical emission may be associated with its activity), and upper limits exist for 17. There is no evident correlation of [N II] equivalent width with L_X. Many clusters of galaxies that are thought to contain cooling flows have filaments with strong [N II] emission (e.g., Hu, Cowie, and Wang 1985; Fabian, Nulsen, and Canizares 1984, and references therein), and it is possible that some of the [N II] emission in early-type galaxies is associated with cooling flows (see below; FJT). More data and more detailed comparisons are required to investigate this question.

A preliminary investigation of the *IRAS* data base shows that a dozen of the galaxies in our sample have detectable far-infrared fluxes, and another six have upper limits. However, there is no evident correlation between the infrared and X-ray properties. Consideration of the implications of this on the possible star formation rates in galaxy cooling flows is beyond the scope of this paper.

d) *Presence of Neutral Hydrogen*

Measurements of the mass of H I ($M_{\rm H\,I}$) are available for 15 galaxies in our sample from the works of Knapp, Turner, and Cunniffe (1985) and Wardle and Knapp (1986). There are upper limits for 43 galaxies. Plots of $M_{\rm H\,I}/L_B$ versus L_X show no correlations or systematic trends. If most of the H I is of external origin, as suggested by these authors, then no correlations would be expected. We note, however, that a hot intergalactic medium would have an important effect on mechanisms for stripping neutral gas from dwarf companions and on its subsequent lifetime.

V. PHYSICAL PROPERTIES OF THE HOT GAS

X-ray data can be used to derive the physical properties of the gas, such as central density, cooling time, and total mass. This has been done for the $\sim$15 galaxies with data of sufficient quality to allow detailed studies of the radial distribution of the gas; approximate temperatures can be measured for about half of these (FJT; Stanger and Schwarz 1986; TFC). Despite significant galaxy to galaxy variations, there is sufficient similarity in the measured profiles to adopt a generic form for the X-ray surface brightness that plays a role analogous to that of the "King law" for optical profiles. This is

$$S(r) = S(0)[1 + (r/a_X)^2]^{-1}\,, \tag{3}$$

where r is the radius and a_X is the core radius. The mean temperatures are all consistent with $\sim 10^7$ K, although most are not very well constrained and the full range is $\sim$0.5–4×10^7 K.

We have deduced approximate values of the physical parameters of the X-ray emitting gas for the galaxies in our sample by assuming that they all have radial profiles given by equation (3). This implies an electron density in the gas of

$$n_e(r) = n_e(0)[1 + (r/a_X)^2]^{-3/4}\,. \tag{4}$$

The volume emission measure is

$$\epsilon = \int n_e^2\, dV\,,$$

$$\epsilon = 4\pi n_e(0)^2 a_X^3[\ln(2R_X/a_X) - 1]\,, \tag{5}$$

where R_X is the maximum radial extent of the gas, and we assume $R_X \gg a_X$. Equation (5) can be used to give an approximate expression for the central density $n_e(0)$ and central cooling time $\tau(0)$ in terms of the observed total luminosity of the galaxy L_X (on the assumption that it is all thermal),

$$n_e(0) = 0.061(L_X/10^{41}\ \text{ergs s}^{-1})^{1/2}(a_X/1\ \text{kpc})^{-3/2}\ \text{cm}^{-3}\,, \tag{6}$$

$$\tau(0) = 1.1 \times 10^8(L_X/10^{41}\ \text{ergs s}^{-1})^{-1/2} \times (a_X/1\ \text{kpc})^{3/2}(T/10^7\ \text{K})\ \text{yr}\,. \tag{7}$$

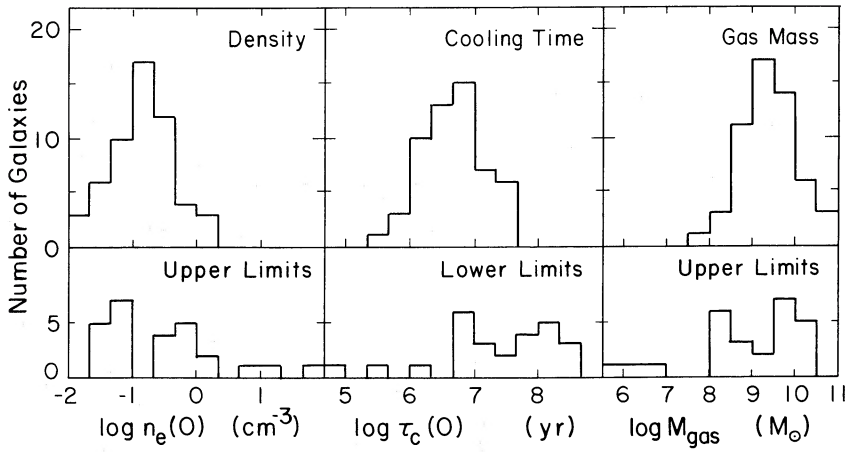

FIG. 3.—Histograms of the estimated central electron density $n_e(0)$, cooling time $\tau(0)$, and total gas mass within 50 core radii M_{gas}. In each case, the upper panels show detections and the lower panels show limits.

Here we have taken a plasma emissivity of 2×10^{-23} ergs cm^3 s^{-1} (Mewe and Gronenschild 1981), and we arbitrarily choose

$$R_X = 50 a_X \, . \tag{8}$$

The total mass of the gas is

$$M_{gas} \approx 8\pi/3 \; 1.2 m n_e(0) (a_X R_X)^{3/2}$$
$$= 5.0 \times 10^9 (L_X/10^{41} \text{ ergs s}^{-1})^{1/2} (R_X/50 \text{ kpc})^{3/2} M_\odot \, . \tag{9}$$

We have assumed that $T = 10^7$ K, which is probably valid to a factor of 2–3. The X-ray core radius is measured for only a few relatively bright galaxies (FJT; TFC). It is generally not well constrained by low-resolution measurements, while the high-resolution measurements of TFC give core radii roughly comparable to those measured in the optical. There is some evidence for correlations between optical luminosity and both the effective radius and core radius of the optical profiles in elliptical galaxies (see Kormendy 1982). Assuming that this reflects a similar trend in the core radius of the underlying potential and hence in the X-ray profile, we adopt the relation

$$a_X = 1.0 (L_B/10^{11} L_B)^{0.8} \text{ kpc} \, . \tag{10}$$

In Figure 3 we show histograms of the deduced values of $n_e(0)$, $\tau(0)$, and M_{gas} for the detected galaxies in the sample and histograms of upper or lower limits for the undetected galaxies. The typical central densities are ~ 0.1 cm^{-3}, typical central cooling times are $\sim 5 \times 10^6$ yr, and typical gas masses are $5 \times 10^9 M_\odot$. Given our several assumptions, the values for any single galaxy are probably accurate only to factors of 2–4 (agreement with the several more detailed measurements is of this order), but they should give a reasonable representation of the properties of the sample.

VI. COOLING FLOWS IN EARLY-TYPE GALAXIES

The observed high X-ray luminosities and corresponding high gas densities for some galaxies rule out the possibility that the observed gas is flowing out of the galaxy in a sonic wind, because the mass supply from normal stellar processes falls several orders of magnitude short of that required to replenish such a wind (Nulsen, Stewart, and Fabian 1984; very subsonic winds are not stable—A. C. Fabian, private communication). Nulsen, Stewart, and Fabian (1984; also Canizares 1981) suggested instead that cooling flows similar to those found in clusters of galaxies (Fabian, Nulsen, and Canizares 1984) are operating in early-type galaxies. White and Chevalier (1984) and more recently Fabian, Arnaud, and Thomas (1986) have computed detailed models of steady flows in galaxies. The very short central cooling times of Figure 3 indicate that all galaxies in the sample having detectable gaseous components could have cooling flows.

The possible sources of heat for gas in early-type galaxies are supernova explosions and gravitational processes (Mathews and Baker 1971; McDonald and Bailey 1981; White and Chevalier 1983, 1984). Here we examine each of these in relation to the observed properties of our sample. Relativistic electrons are a potential source of heat, but it is unlikely that it dominates; X-ray luminosity is less tightly correlated with radio luminosity than with optical luminosity, radio lobes are often smaller than the extent of the X-ray emitting gas and are often much less symmetric, and the total energy in the radio lobes is generally less than that in the gas (see, e.g., Stanger and Warwick 1986; Fabbiano *et al.* 1987).

a) Heating by Supernovae

The supernova rate, and therefore the power from supernovae, should be roughly proportional to the optical luminosity of a galaxy (Tammann 1974). Assuming an energy of 10^{51} ergs per supernova, the power would be

$$L_{SN} = 7.1 \times 10^{41} (R_{SN}/0.22)(L_B/10^{11}) \text{ ergs s}^{-1} \, , \tag{11}$$

where R_{SN} is the supernova rate per (10^{10} L_B 100 yr). Standard models predict that all this energy is deposited in the low-density, high-pressure gas and therefore will be radiated primarily as X-rays (see Chevalier 1974; McKee and Ostriker 1977; in the models of White and Chevalier 1984, only galaxies with $L_B < 10^9$ are too cool to radiate X-rays).

Equation (11) is plotted in Figures 1 and 2 as a short-dashed curve. We have normalized to $R_{SN} = 0.22$, which is the rate deduced by Tammann (1982) from observations of a dozen supernovae in elliptical galaxies (his estimate of the rate in S0's is one-half the rate in ellipticals; see also Oemler and Tinsley 1979). The figures show that L_{SN} exceeds the observed X-ray luminosity of all but the most luminous galaxies by factors up to 20. It is intriguing that the L_{SN} curve appears to define an upper boundary to the distribution at the high-L_X end.

Because in general $L_X \ll L_{SN}$, we conclude that in most early-type galaxies either the supernova rate is significantly lower than Tammann's estimate (see also Sarazin 1986; Fabian, Arnaud, and Thomas 1986; Thomas 1986) or the bulk of the supernova energy does not appear as heat but rather is dissipated or radiated outside the X-ray band. (The latter is thought to occur in spiral galaxies, but the mechanisms require a much denser medium than exists in early-type galaxies; see Cox 1981, 1983). If it is not a coincidence that $L_X \approx L_{SN}$ for some galaxies and that none have $L_X \gg L_{SN}$, then it might suggest that Tammann's rate is correct, and the latter explanation would be favored.

A second consideration if supernova heating dominates is the suppression of a galactic wind. Two possible conditions that can cause gas to flow predominantly inward rather than outward are (1) the cooling time in the core is sufficiently short compared to the flow time to prevent establishment of a wind throughout the galaxy (Mathews and Baker 1971; Bregman 1978; McDonald and Bailey 1981) or (2) the gas lacks sufficient energy to escape the gravitational potential of the galaxy. In the former case, a partial wind is possible.

Condition (1) for dynamical suppression of a wind is

$$\tau(0) < 3R_g/v_{\rm flow} < 3 \times 10^7 (R_g/1\ {\rm kpc})(100\ {\rm km\ s^{-1}}/v_{\rm flow})\ {\rm yr}\ , \quad (12)$$

where R_g is the scale height of the gravitational field and $v_{\rm flow}$ is the flow velocity (Mathews and Baker 1971). Examination of Figure 3 suggests that this condition is marginally satisfied in some galaxies but may not be met in general. In any case, this condition cannot suppress the formation of a wind in the outer parts of the galaxy.

Condition (2) cannot be satisfied in the cores of most galaxies if supernova heating is the dominant source of energy for the gas. In that case the critical temperature above which a wind would be energetically allowed (though not required) is

$$T_{\rm crit} = [(2\mu mG)/(5k)](1/M_*) \int [M_{\rm tot}(<r) M_*(<r) dr/r^2] \quad (13)$$

(J. Bregman, private communication). Here μm is the mean gas particle mass, M_* is the stellar mass in the galaxy, $M_{\rm tot}(<r)$ and $M_*(<r)$ are the total and stellar masses within radius r respectively, which are equal if the galaxy contains no dark matter (G and k are Newton's and Boltzmann's constants respectively). This expression, which is equivalent to equation (18) of McDonald and Bailey (1981), is independent of the supernova rate so long as it is the dominant source of heat. The quantity $T_{\rm crit}$ is less than the escape temperature for the potential, because the gas is continually heated as it moves out through the galaxy. For a galaxy with no halo and with stellar mass $M_* = M_{11}\ 10^{11}\ M_\odot$ distributed like a King law (density $\sim[1 + (r/a_*)^2]^{-3/2}$), equation (13) gives $T_{\rm crit} \approx 1 \times 10^6\ M_{11}\ K$. If a galaxy has a dark, "isothermal" halo with density $\sim[1 + (r/a_h)^2]^{-1}$ and with $M_{\rm tot} = 10\ M_*$, then $T_{\rm crit} \approx 3$–$4 \times 10^6\ M_{11}$ K (the result depends weakly on a_h and the maximum radius of the halo). A galaxy with a very centrally concentrated halo of mass $10\ M_*$, one that follows a King law with core radius $= 5a_*$, has $T_{\rm crit} \approx 7 \times 10^6\ M_{11}$ K. These values fall below most of the observed temperatures quoted above.

These arguments suggest that if the observed X-ray temperatures were achieved primarily as a result of supernova heating, then the required suppression of galactic winds would have to be caused by some external agency, such as the pressure of additional circumgalactic material (note that the models of White and Chevalier 1984 that include supernova heating have finite pressures at the outer boundaries). Recently Mathews and Loewenstein (1986) have suggested that such material might come from a galactic wind trapped in a galaxy halo during an early evolutionary phase of high mass loss.

b) *Heating by Gravitational Processes*

If the gas is primarily heated by gravitational processes, then it will be bound. The observed temperatures are generally less than the temperature corresponding to the depth of the central potential, which for a King law is $(18\ \mu{\rm m}\ \sigma^2)/3k = 1.7 \times 10^7 (\sigma/200\ {\rm km\ s^{-1}})^2$, where σ is the line-of-sight velocity dispersion in the galaxy. Galaxies with heavy halos can have still higher central escape temperatures for the same velocity dispersion.

Gravitational heating includes both thermalization of the gas to the stellar velocity and heating of the gas as it falls through the potential of the galaxy (e.g., White and Chevalier 1984). Thus we can express the average energy input per gram as

$$E_g = 3\sigma^2/2 + f\langle\Delta\Phi\rangle_m \quad (14)$$

(see also Sarazin 1986). Here

$$\langle\Delta\Phi\rangle_m = (1/M_*)_0 \int^{M_*} \Delta\Phi dM_* \quad (15)$$

is the average potential difference through which gas falls, appropriately weighted by the distribution of stellar mass and therefore injected mass, and f is a factor less than or equal to 1 which allows for the possibility that the mass does not fall all the way to the center of the galaxy. Equation (15) can be evaluated to give

$$\langle\Delta\Phi\rangle_m = 6.9A\sigma^2\ , \quad (16)$$

where A is a constant that depends on the properties of the galaxy potential. For a King law, $A = 1$. If the galaxy has a dark halo, then $A \approx 2$–4 (the higher value is for an isothermal halo with 10 times the stellar mass).

With equations (14) and (16) we can relate the gravitational heating rate to L_B and σ^2,

$$\begin{aligned} L_{\rm grav} &= \dot{m}(1.5 + 6.9fA)\sigma^2 \\ &= \alpha(1.5 + 6.9fA)L_B\sigma^2 \\ &= 3.9 \times 10^{39}(1.5 + 6.9fA) \\ &\quad \times (L_B/10^{10}L_\odot)(\sigma/200\ {\rm km\ s^{-1}})^2\ . \end{aligned} \quad (17)$$

Here $\dot{m}$ is the rate of mass injection from normal stellar processes, which is proportional to L_B with proportionality constant α. Faber and Gallagher (1976) estimated α to be $\sim 0.15\ M_\odot\ {\rm yr}^{-1}\ (10^{10}\ L_\odot)^{-1}$, and we have used this value in equation (17).

In a steady state, gravitationally dominated flow, $L_{\rm grav}$ would be the bolometric luminosity of the gas, but for many galaxies, the gas would be too cool to emit X-rays. The peak temperature of a gravity-dominated cooling flow is related to the depth of the gravitational potential Φ_0 and only weakly dependent on its shape. For a King law

$$T_{\rm max} \approx 0.16\ \mu m\Phi_0/k \quad (18)$$

(see Fig. 8 of Fabian, Nulsen, and Canizares 1984; note that the maximum temperatures of the White and Chevalier 1984 models in the regions where gravity dominates follow eq. [18]).

For reasonable assumptions about the potential (with or without a halo), flows in galaxies with optical luminosities $L_B \leq 10^{10}\ L_\odot$ would have temperatures below 5×10^6 K and therefore would have significantly lower apparent luminosities in the *Einstein* band.

Equation (17) can be compared to the data by using the observed relationship between optical luminosity and σ (Faber and Jackson 1976; also Tonry 1981). Nulsen, Stewart, and Fabian (1984) used this to predict that $L_X \propto L_B^{1.5}$, which is reasonably close to what is observed (TF and Table 3). However, the L_B versus σ relation itself has considerable scatter, so we have computed $L_B\sigma^2$ directly for all those galaxies in the sample with measured velocity dispersions (taken from the compilation of Whitmore, McElroy, and Tonry 1985). The values are listed in Table 1.

In Figures 4 and 5 we show L_X and ΔL_X respectively, plotted against $L_B\sigma^2$. Also shown in Figure 4 is the curve for $L_{\rm dscr}$ from Figure 1, transformed using the relation between L_B and σ from Tonry (1981) corrected to our assumed Virgo distance. We fit the distributions of the data in these figures using the method described in § IV*b*. The results are listed in Table 3. All the fits are consistent with a linear relationship between the X-ray luminosity and $L_B\sigma^2$ (i.e., $b \approx 1$).

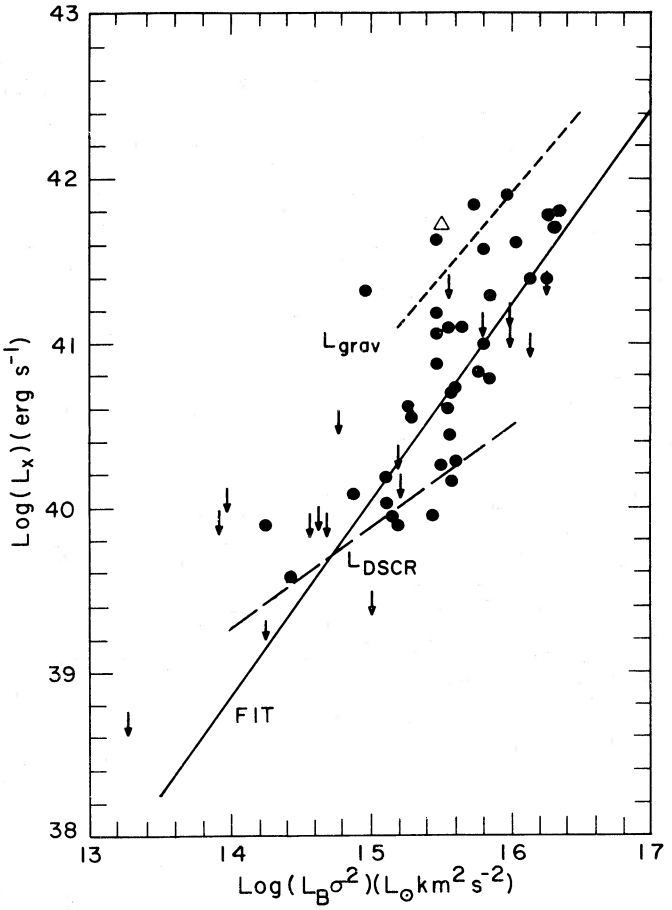

FIG. 4.—X-ray luminosity vs. the product $L_B\sigma^2$ for the full sample of early-type galaxies. The symbols are as in Fig. 1. The long-dashed curve represents $L_{\rm dscr}$ as described in the text. The solid curve is the fit to the mean of the distribution. The short-dashed curve is $L_{\rm grav}$, the energy available from gravitational heating according to eq. (17) (with $fA = 1$), which is drawn only for higher values of $L_B\sigma^2$ at which the temperatures in gravitationally dominated flows are sufficiently high to give X-rays.

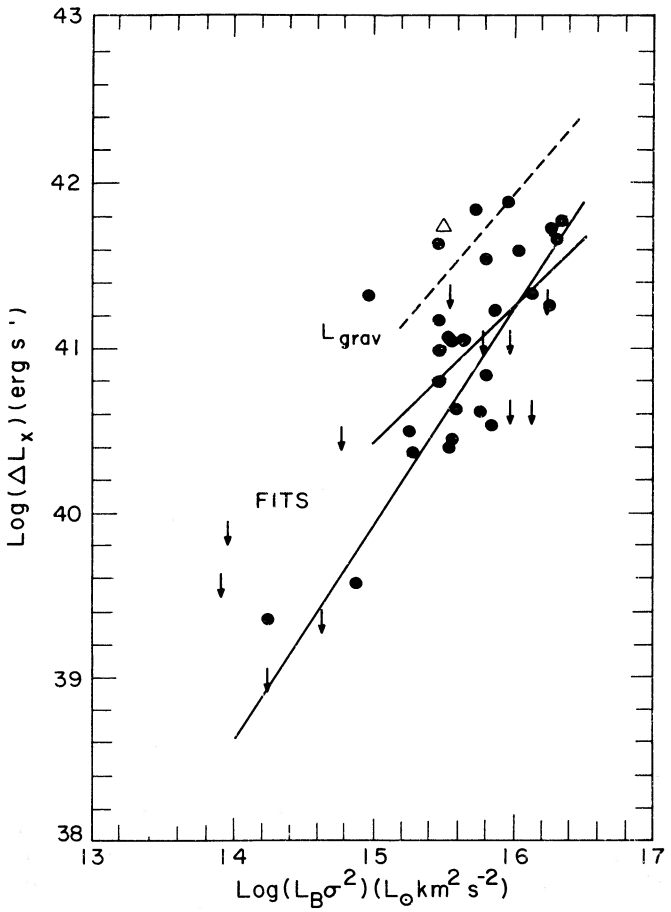

FIG. 5.—ΔL_X vs. $L_B\sigma^2$. The symbols are as in Fig. 1, and the curve marked $L_{\rm grav}$ is as in Fig. 4. The longer of the two solid lines is the fit from Table 3 for the full sample, and the shorter solid line is the fit to the subsample that excludes the galaxies in Table 2.

Figures 4 and 5 show the relation of equation (17) for the case $fA = 1$. The curve extends only over the region for which one would expect $L_{\rm grav} \approx L_X$. This corresponds roughly to the range of $L_b\sigma^2$ that is populated by the galaxies with moderate to high values of ΔL_X. Also, the linearity of L_X with $L_b\sigma^2$ in equation (17) is consistent with the best-fit slopes of the distributions in Table 3. On the other hand, equation (17) gives X-ray luminosities about a factor of 3–4 above the best-fit mean. This could be reconciled if the mean α were smaller than the estimate of Faber and Gallagher (1979), which is probably uncertain to this order (S. Faber, private communication), if a considerable fraction of $\dot{m}$ were not incorporated into the flow, or if mass is removed from the flow before it has fallen to the center of the galaxy (i.e., $fA \leq 0.3$). A detailed analysis of the X-ray data for NGC 4472 by Thomas (1986) suggests that both may be true.

c) Conclusions

Presumably both supernova heating and gravitational heating are taking place in early-type galaxies. With accepted values of the parameters, each process alone would overproduce the observed X-ray luminosity for most galaxies, and so mechanisms for reducing the heat input, such as those we have suggested, must exist. It is not possible to know which heating process dominates without understanding the details

of those mechanisms. Whatever mechanisms are invoked, they must also be capable of explaining the large scatter in the L_X versus L_B distribution. At present we have found no observational parameter that distinguishes a high-L_X from a low-L_X galaxy with similar L_B. One process that could contribute to the scatter is stripping of galactic gas by intracluster gas (e.g., Takeda, Nulsen, and Fabian 1984). Some of the Virgo galaxies may have been affected by such stripping (Forman, Jones, and DeFaccio 1984).

VII. IMPLICATIONS FOR THE EXISTENCE OF HEAVY HALOS

Studies of the detailed X-ray properties of early-type galaxies can be used to map their gravitational potentials and thus indicate the presence and extent of possible heavy halos (FJT; TFC; Fabian, Arnaud, and Thomas 1986; Canizares 1986). Our analysis of the global X-ray properties shows that these are *not* particularly sensitive to the presence or absence of heavy halos. The halos manifest themselves primarily in the radial distribution of the X-ray properties, particularly the behavior at large radii, and only slightly in their integrated properties (such as the factor A in eqs. [15] and [16] or the small variations in $T_{\rm crit}$). Thus, the presence of hot gas in early-type galaxies is itself not sufficient evidence for halos.

It is possible to make one indirect inference. If gravitational processes do dominate the heating of the gas, then a King law potential would give much more centrally peaked X-ray surface brightness profiles than are observed: at large radii $S(r) \propto r^{-3}$ rather than r^{-2} (see eq. [13]). However, even the addition of a modest "isothermal" halo (e.g., with mass $\sim 3M_*$) could flatten the distribution and make it consistent with equation (3). Injection of energy from supernovae at large radii and transport of heat by conduction could also be important (see White and Chevalier 1984; TFC; Fabian, Nulsen, and Canizares 1984; Rosner, Tucker, and Nijita 1986; Thomas 1986).

It will be some time before new X-ray data on elliptical galaxies can be acquired. Until then, detailed modeling of the brightest and best studied galaxies with a wide range of assumptions is required to understand the properties of the gas, to constrain further the possible heating mechanisms and the reasons for the suppression of winds, and to address the question of heavy halos.

We have had useful conversations with Jill Bechtold, Joel Bregman, Andy Fabian, John Huchra, Bill Mathews, Paul Nulsen, Craig Sarazin, and Peter Thomas. We thank Joel Bregman for communicating his $T_{\rm crit}$ calculation, and Roger Davies for information about Cen A. We are grateful to John Huchra for providing us with radial velocities and with his Virgocentric flow model. We thank Julia White for assistance with the data analysis, and the referee for helpful comments. Part of this work was performed while C. R. C. was a guest of the Institute of Astronomy, University of Cambridge, and he thanks them for their hospitality. This work was supported in part by NASA contract NAS8-30751 and grant NAG8-494.

REFERENCES

Aaronson, M., Huchra, J., Mould, J., Schechter, P., and Tully, R. B. 1982, *Ap. J.*, **258**, 64.
Allen, C. W. 1973, *Astrophysical Quantities* (3d ed.; London: Athlone).
Avni, Y., Soltan, A., Tananbaum, H., and Zamorani, G. 1980, *Ap. J.*, **238**, 800.
Bechtold, J., Forman, W., Giacconi, R., Jones, C., Schwarz, J., Tucker, W., and Van Speybroeck, L. 1983, *Ap. J.*, **265**, 26.
Biermann, P., and Kronberg, P. P. 1983, *Ap. J. (Letters)*, **268**, L69.
Biermann, P., Kronberg, P. P., and Madore, B. F. 1982, *Ap. J. (Letters)*, **256**, L37.
Bohlin, R. C., Cornett, R. H., Hill, J. K., Hill, R. S., O'Connell, R. W., and Stecher, R. P. 1985, *Ap. J. (Letters)*, **298**, L37.
Bregmann, J. 1978, *Ap. J.*, **244**, 768.
Bridle, A. H., and Fomalont, E. B. 1978, *A.J.*, **83**, 704.
Canizares, C. R. 1981, in *X-ray Astronomy with the Einstein Observatory*, ed. R. Giacconi, (Dordrecht: Reidel). p. 215.
———. 1986, in *IAU Symposium 117, Dark Matter in the Universe*, ed. J. Kormendy and G. Knapp (Dordrecht: Reidel), in press.
Canizares, C. R., Donahue, M., Trinchieri, G., Stewart, G., and McGlynn, T. 1986, *Ap. J.*, **304**, 312.
Chevalier, R. 1974, *Ap. J.*, **188**, 501.
Cox, D. P. 1981, *Ap. J.*, **245**, 534.
———. 1983, in *Supernova Remnants and Their X-Ray Emission*, ed. J. Danziger and P. Gorenstein (Dordrecht: Reidel), p. 385.
Davies, R. L., Danziger, J., Fabian, A., Hanes, R., Jones, B., Jones, J., Morton, D., and Pennington, R. 1984, *Bull. AAS*, **16**, 410.
de Vaucouleurs, G., and Pence, W. D. 1979, *Ap. J. Suppl.*, **39**, 79.
de Vaucouleurs, G., de Vaucouleurs, A., and Corwin Jr., H. G. 1976, *Second Reference Catalog of Bright Galaxies* (Austin: University of Texas Press) (RC2).
Dressel, L., and Wilson, A. 1985, *Ap. J.*, **291**, 668.
Dufour, R. J., van den Bergh, S., Harvel, C., Martins, D., Schiffer, F. H., Talbot, Jr., R. J., Talent, D. L., and Wells, D. C. 1979, *A.J.*, **84**, 284.
Elvis, M., Schreier, E. J., Tonry, J., Davis, M., and Huchra, J. P. 1981, *Ap. J.*, **246**, 20.
Fabbiano, G., Klein, U., Trinchieri, G., and Wielebinski, R. 1987, *Ap. J.*, **312**, in press.
Fabbiano, G., Miller, L., Trinchieri, G., Longair, M., and Elvis, M. 1984, *Ap. J.*, **277**, 115.
Fabbiano, G., and Trinchieri, G. 1985, *Ap. J.*, **296**, 430.
Fabbiano, G., Trinchieri, G., and van Speybroeck, L. 1986, in preparation.
Faber, S. 1983, in *Highlights Astr.*, **6**, 165.
Faber, S., and Gallagher, J. 1976, *Ap. J.*, **204**, 365.
———. 1979, *Ann Rev. Astr. Ap.*, **17**, 135.
Faber, S., and Jackson, R. E. 1976, *Ap. J.*, **204**, 668.
Fabian, A. C., Arnaud, K., and Thomas, P. 1986, in *IAU Symposium 117, Dark Matter in the Universe*, ed. J. Kormendy, and G. Knapp (Dordrecht: Reidel), in press.
Fabian, A. C., Nulsen, P. E. J., and Canizares, C. R. 1984, *Nature*, **310**, 733.
Feigelson, E., Schreier, E., Delvaille, J., Giacconi, R., Grindlay, J., and Lightman, A. 1981, *Ap. J.*, **251**, 31.
Forman, W., Jones, C., and DeFaccio, M. 1984, in *Proc. ESO Workshop on the Virgo Cluster*, ed. O. G. Richter, and B. Binggeli (Garching: ESO Conf. Proc. 20), p. 323.
Forman, W., Jones, C., and Tucker, W. 1985, *Ap. J.*, **293**, 102 (FJT).
Forman, W., Schwarz, J., Jones, C., Liller, W., and Fabian, A. 1979. *Ap. J. (Letters)*, **234**, L27.
Geller, M., and Huchra, J. 1983, *Ap. J. Suppl.*, **52**, 61.
Hu, E. M., Cowie, L. L., and Wang, Z. 1985, *Ap. J. Suppl.*, **59**, 447.
Huchra, J., and Geller, M. 1982, *Ap. J.*, **257**, 432.
Killeen, N. E. B., Bicknell, G. V., and Carter, D. 1986, preprint.
Killeen, N. E. B., Bicknell, G. V., and Ekers, R. D. 1986, *Ap. J.*, **302**, 306.
Knapp, G. R., Turner, E. L., and Cunniffe, P. E. 1985, *A.J.*, **90**, 454.
Kormendy, J. 1982, in *Morphology and Dynamics of Galaxies*, ed. J. Binney, S. White, and J. Kormendy (Geneva: Geneva Observatory), p. 113.
Mathews, W., and Baker, J. 1971, *Ap. J.*, **170**, 241.
Mathews, W. G., and Loewenstein N. 1986, *Ap. J. (Letters)*, **306**, L7.
McDonald, J., and Bailey, M. 1981, *M.N.R.A.S.*, **197**, 995.
McKee, C., and Ostriker, J. 1977, *Ap. J.*, **218**, 148.
Mewe, R., and Gronenschild, B. M. 1981, private communication.
Nilson, P. 1973, *Uppsala General Catalogue of Galaxies* (Uppsala: Uppsala University).
Nulsen, P. E. J., Stewart, G. C., and Fabian, A. C. 1984, *M.N.R.A.S.*, **208**, 185.
Oemler, G., Jr., and Tinsley, B. M. 1979, *A.J.*, **84**, 985.
Oke, J. B., Bertola, F., and Capaccioli, M., 1981, *Ap. J.*, **243**, 453.
Phillips, M. M., Jenkings, C. R., Dopita, M. A., Sadler, E. M., and Binette, L. 1985, preprint.
Press, W., and Schechter, P. 1974, *Ap. J.*, **193**, 437.
Rosner, R., Tucker, W., and Nijita, J. 1986, preprint.
Sandage, A., and Tammann G. 1981, *A Revised Shapley-Ames Catalog of Bright Galaxies*, (Washington, D. C.: Carnegie Institution of Washington) (RSA).
Sarazin, C. 1986, in *IAU Symposium 117, Dark Matter in the Universe*, ed. J. Kormendy and G. Knapp, (Dordrecht: Reidel) in press.
Stanger, V. J., and Schwarz, J. 1986, *Ap. J.*, submitted.
Stanger, V. J., and Warwick, R. S. 1986, *M.N.R.A.S.*, **220**, 363.
Takeda, H., Nulsen, P. E. J., and Fabian, A. C. 1984, *M.N.R.A.S.*, **208**, 261.

Tammann, G. 1974, in *Supernovae and Supernova Remnants*, ed. C. B. Cosmovici (Dordrecht: Reidel, p. 155.
———. 1982, in *Supernovae: A Survey of Current Research*, ed. M. Reese and R. Stoneham (Dordrecht: Reidel), p. 371.
Tammann, G., and Sandage, A. 1985, *Ap. J.*, **294**, 81.
Thomas, P. 1986, *M.N.R.A.S.* in press.
Tonry, J. 1981, *Ap. J.* (*Letters*), **251**, L1.
Trinchieri, G., and Fabbiano, G. 1985, *Ap. J.*, **296**, 447 (TF).
Trinchieri, F., Fabbiano, G., and Canizares C. 1986, *Ap. J.*, **310**, 637 (TFC).
Véron-Cetty, M.-P., and Véron, P. 1985, preprint.
Wardle, M., and Knapp, G. R. 1986, *A.J.*, **91**, 23.
White, R. E., and Chevalier, R. A., 1983, *Ap. J.*, **275**, 69.
———. 1984, *Ap. J.*, **280**, 561.
Whitmore, B. C., McElroy, D. B., and Tonry, J. L. 1985, *Ap. J. Suppl.*, **59**, 1.
Zwicky, F., *et al.* 1968, *Catalog of Galaxies and Clusters of Galaxies*, (Pasadena: Cal. Tech).

CLAUDE R. CANIZARES: Room 37-501, MIT, Cambridge, MA 02139

GIUSEPPINA FABBIANO: Center for Astrophysics, 60 Garden St., Cambridge, MA 02138

GINEVRA TRINCHIERI: Osservatorio Astrofisico di Arcetri, Largo Enrico Fermi 5, 150125, Firenze, Italy